0026-895X/01/6003-620–628$3.00
MOLECULAR PHARMACOLOGY
Copyright © 2001 The American Society for Pharmacology and Experimental Therapeutics
Mol Pharmacol 60:620–628, 2001

Vol. 60, No. 3
1002/928558
Printed in U.S.A.

A Phenylalanine Residue at Segment D3-S6 in Nav1.4 Voltage-Gated Na^+ Channels Is Critical for Pyrethroid Action

SHO-YA WANG, MARIA BARILE, and GING KUO WANG

Department of Biological Sciences, State University of New York at Albany, New York (S.Y.W.); Department of Anesthesia, Harvard Medical School and Brigham and Women's Hospital, Boston, Massachusetts (M.B., G.K.W.)

Received April 4, 2001; accepted June 12, 2001

This paper is available online at http://molpharm.aspetjournals.org

ABSTRACT

Mammalian voltage-gated Na^+ channels were less sensitive to pyrethroids than their insect counterparts by 2 to 3 orders of magnitude. Deltamethrin at 10 μM elicited weak gating changes in rat skeletal muscle α-subunit Na^+ channels (Nav1.4) after $>$ 30 min of perfusion. About 10% of the peak current was maintained during the 8-ms, +50-mV pulse and, upon repolarization to −140 mV, the amplitude of the slow tail current corresponded to less than 3% of total Na^+ channels modified by deltamethrin. A background mutation, Nav1.4-I687M (within D2:S4-S5 cytoplasmic linker), enhanced the deltamethrin-induced maintained current by ~2.5-fold, whereas Nav1.4-I687T, a homologous *superkdr* mutation, reduced it by ~2-fold. Repetitive pulses at 2 Hz further augmented the effects of deltamethrin on Nav1.4-I687M mutant channels so that ~75% of peak currents were maintained. A second mutation, Nav1.4-I687M/F1278I at the middle of D3-S6, rendered the channel greatly resistant to deltamethrin. This double mutant channel remained sensitive to batrachotoxin (BTX), even though nearby residues S1276 and L1280 were critical for BTX action. We hypothesize that the deltamethrin receptor and the BTX receptor are situated at the middle but opposite surface of the D3-S6 α-helical structure. Another mutant, Nav1.4-I687M/N784K, exhibited a partial deltamethrin-resistant phenotype but was completely resistant to BTX. Consistent with the BTX-resistant phenotype of N784K and the known adjacent *kdr* mutation at position L785F, deltamethrin and BTX were probably situated next to each other upon binding at D2-S6. Evidently, distinct residues from multiple S6 segments were critical for deltamethrin and BTX actions.

Pyrethroid insecticides are synthetic analogs of the naturally occurring ingredients found in certain chrysanthemum flowers (Narahashi, 1992; Zlotkin, 1999). They are widely used in the control of the insect population for crop protection and for pest-related diseases. Over the last 2 decades, however, many wild insect species have become resistant to pyrethroids. One type of pyrethroid resistance involves the genetic alternation of the voltage-gated Na^+ channel gene. The *knockdown* resistant and *superknockdown* resistant phenotypes (*kdr* and *superkdr* resistance) among houseflies are two examples (Bloomquist and Miller, 1986; Pauron et al., 1989). Sequence analyses of pyrethroid-resistant houseflies (e.g., *Musca domestica*; Williamson et al., 1996) and other insect species (e.g., German cockroaches; Miyazaki et al., 1996) have identified position L1014F of the insect *para* Na^+ channel gene as the common "defective" site for their *kdr* phenotypes. The *kdr* defect is caused by *para*-L1014F mutation, whereas the *superkdr* defect is caused by two mutations of both *para*-L1014F and *para*-M918T.

Wild-type insect Na^+ channels are readily modified by pyrethroids at submicromolar concentrations (Vais et al., 2000a); their fast inactivation is severely hampered and incomplete during depolarization. Because the pyrethroid-modified open Na^+ channel cannot be shut off upon membrane repolarization, a tail current that lasts for several seconds appears at the holding potential. It is feasible to study pyrethroid effects directly using *Drosophila melanogaster para* Na^+ channels expressed in *Xenopus laevis* oocytes (Warmke et al., 1997). The *kdr* and *superkdr* mutations in the *para* Na^+ channel reduce the binding affinity of the pyrethroid deltamethrin (for structure see Fig. 1) by 20- and 100-fold, respectively (Vais et al., 2000a), and dose-response studies suggest that the stoichiometry for pyrethroid binding is about two per *para* channel. At present, despite serious efforts, the *para* Na^+ channels have not been expressed in mammalian expression systems.

The α-subunit Na^+ channel protein consists of four repeated domains, each with six transmembrane segments (Catterall, 2000). The physical location of *para*-L1014F (*Musca domestica*) within the α-subunit Na^+ channel protein is near the middle of the D2-S6 segment (Fig. 1). The four S6 transmembrane segments may bundle together as an inverted teepee and the middle sections of the S6 segments

This study was supported by National Institutes of Health Grants GM35401 and GM48090.

ABBREVIATIONS: *kdr,* knockdown resistance; *superkdr*, superknockdown resistance; BTX, batrachotoxin; HEK, human embryonic kidney.

probably encircle the internal vestibule of the channel permeation pathway (Doyle et al., 1998; Lipkind and Fozzard, 2000; Wang et al., 2000). Recently, a PCR-mapping study provided genetic evidence that a novel Na^+ channel point mutation in the cattle tick *Boophilus micropuls* is present in two field strains that are resistant to pyrethroid (He et al., 1999). This point mutation is located near the middle of the D3-S6 segment. The insecticide-resistant phenotype of this point mutation has not yet been studied at the cellular level and the tick Na^+ channel has not been determined in its entirety.

We and others previously proposed that the middle sections of multiple S6 segments form a receptor site for batrachotoxin (BTX) (Fig. 1B; highlighted; Linford et al., 1998; Wang and Wang, 1998; Wang et al., 2000; 2001). In addition, these four S6 segments probably align in close proximity along the permeation pathway, particularly when the channel is in its inactivated state (Wang et al., 2001). Pyrethroids and BTX are Na^+ channel activators, which cause Na^+ channels to open more easily and stay open longer than normal (Hille, 1992). To account for the pharmacological effects induced by both pyrethroids and batrachotoxin (for structure, see Fig. 1), it seems reasonable to hypothesize that the residue within D3-S6 identified by He et al. (1999) and the residue from D2-S6 identified in *kdr* houseflies form a part of the pyrethroid receptor.

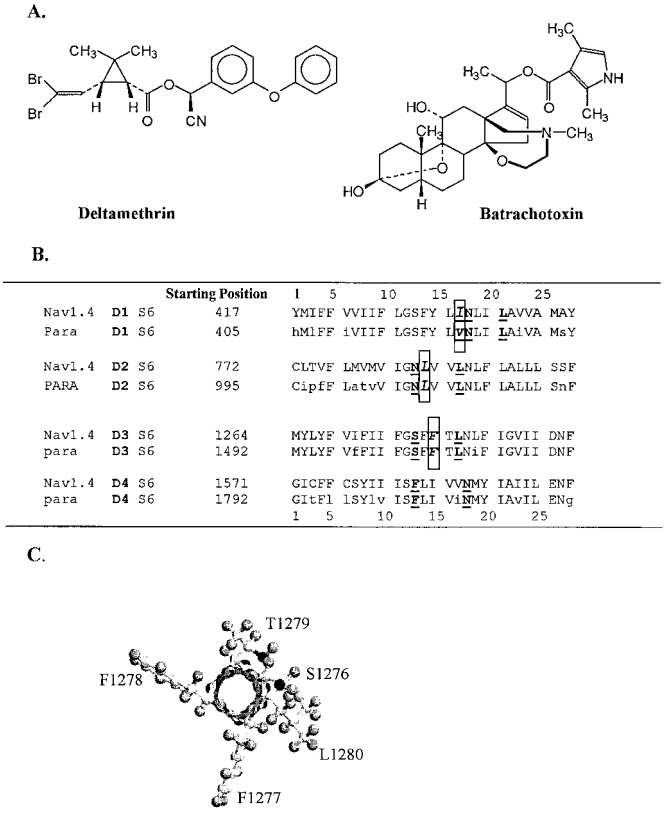

Fig. 1. A, chemical structures of deltamethrin (505 Da) and batrachotoxin (538 Da). B, sequence alignment of S6 segments from D1 to D4 in rat Nav1.4 and *para* Na^+ channels (*D. melanogaster*). Underlined bold letters represent residues critical for batrachotoxin action. Boxed bold letters depict residues critical for deltamethrin action. C, relative positions of S1276, F1277, F1278, T1279, and L1280 on the Nav1.4-D3-S6 α-helical structure; view from top to bottom using Alchemy 2000 (Tripos, Inc. St. Louis, MO).

We used a mammalian expression system to inquire (1) whether a corresponding point mutation at D3-S6 in the rat skeletal muscle Na^+ channel (Nav1.4-F1278I) will render this mutant resistant to deltamethrin, as predicted from the above hypothesis, and (2) whether the BTX receptor and the deltamethrin receptor overlap. Unfortunately, the pyrethroid potencies in insect and mammalian Na^+ channels differ significantly (Narahashi, 1992). To exploit mammalian Nav1.4 channels for the insecticide study, we created a homologous point mutation (Nav1.4-I687M) at the D2:S4–S5 intracellular linker, which increases the pyrethroid affinity (e.g., Nav1.2 in oocytes, Vais et al., 2000a). Such a point mutation is unlikely to reproduce all the features of the *para* isoform. Our results nonetheless demonstrate that the Nav1.4-I687M/F1278I mutant channel indeed confers the insecticide-resistant phenotype found in the cattle tick *B. micropuls*. Our data also indicate that receptors for BTX and deltamethrin are structurally distinct, consistent with direct BTX binding studies reported by Lombet et al. (1988) and Trainer et al. (1993).

Materials and Methods

Site-Directed Mutagenesis. Transformer Site-Directed Mutagenesis Kit (CLONTECH, Palo Alto, CA) was used to create Nav1.4 Na^+ channel mutant clones as described previously (Nau et al., 1999). Two primers (a mutagenesis primer and a restriction primer) were used to generate the desired mutant. DNA sequencing near the mutated region confirmed the mutation. Mutants of Nav1.4-I687M, Nav1.4-I687T, Nav1.4-I687M-F1278I, and Nav1.4-I687M-N784K were used along with the wild-type in this study. Mutants of Nav1.4-I687M-L785K, Nav1.4-L785F, and Nav1.4-L785H were prepared but failed to express sufficient Na^+ currents.

Transient Transfection. Human embryonic kidney (HEK) 293t cells were grown to ~50% confluence in Dulbecco's modified Eagle's medium (Invitrogen, Carlsbad, CA) containing 10% fetal bovine serum (HyClone, Logan, UT), 1% penicillin and streptomycin solution (Sigma, St. Louis, MO), 3 mM taurine, and 25 mM HEPES (Invitrogen) and then transfected by a calcium phosphate precipitation method in a Ti25 flask. Transfection of Nav1.4-pcDNA1/Amp (10–20 μg) and reporter plasmid CD8-pih3 m (1 μg) was adequate for later current recording. Cells were replated 15 h after transfection in 35-mm culture dishes, maintained at 37°C in a 5% CO_2 incubator, and used for experiments after 1 to 4 days. Transfection-positive cells were identified by immunobeads (CD8-Dynabeads; Dynal, Lake Success, NY).

Whole-Cell Voltage Clamp. Whole-cell configuration was used to record Na^+ currents in cells coated with CD-8 beads (Hamill et al., 1981; Cannon and Strittmatter, 1993). Pipette electrodes contained 100 mM NaF, 30 mM NaCl, 10 mM EGTA, and 10 mM HEPES adjusted to pH 7.2 with CsOH. The tips of electrodes had a resistance of 0.5 to 1.0 MΩ. All experiments were performed at room temperature (22 to 24°C) under a low Na^+- bath solution containing 65 mM NaCl, 65 mM choline Cl, 2 mM $CaCl_2$, and 10 mM HEPES adjusted to pH 7.4 with tetramethylhydroxide. The benefit of using a low Na^+ external solution was described by Cota and Armstrong (1989) and was applied here to further minimize Na^+ loading caused by persistent opening of BTX-modified and deltamethrin-modified Na^+ channels. Stock solutions of BTX (0.5 mM) and deltamethrin (10 mM) were dissolved in dimethyl sulfoxide. Deltamethrin (purchased from Crescent Chemical Co., Hauppauge, NY) was applied externally at a final concentration of 10 μM. Because of its low solubility, this is the highest deltamethrin concentration that we could apply. The neurotoxin BTX was a generous gift from John Daly (National Institutes of Health, Bethesda, MD). BTX at a final concentration of 5 μM (~500 times of the known dissociation constant value) was included in the

internal pipette solution when needed. Whole-cell currents were measured by a patch-clamp device (EPC-7 or Axopatch 200B), filtered at 5 kHz, collected, and analyzed using pClamp software (Axon Instruments, Foster City, CA). Leak and capacitance were first subtracted by the Axopatch device and further by the pClamp leak subtraction protocol (P/−4). Cells were always held at −140 mV to avoid cumulative fast and slow inactivation in mutant channels during repetitive pulses. Because of the presence of tail currents after deltamethrin treatment, no (P/−4) leak subtraction was implemented during repetitive pulses. An unpaired Student's t test was used to evaluate estimated parameters (means ± S.E.M.); P values of <0.05 were considered statistically significant.

Results

Background Mutation in Rat Skeletal Muscle Na^+ Channels (Nav1.4) for Insecticide Studies. We first constructed a point mutation at position 687 of the S4–S5 intracellular linker within domain D2 in the Nav1.4 Na^+ channel to increase its pyrethroid affinity using HEK293t cells. Figure 2, A and C, shows families of superimposed Na^+ current traces from Nav1.4 wild-type and Nav1.4-I687M mutant channels at various voltages. The wild-type Na^+ currents were activated around −50 to −60 mV and reversed from inward to outward around −12 mV under our ionic conditions. After reaching its peak amplitude, the current decays and reaches the baseline level within the pulse duration. Little or no maintained current is found near the end of the 8-ms pulse at potentials less than +30 mV. Typical modifications in wild-type current kinetics by external deltamethrin at 10 μM are shown after ~45 min of treatment (Fig. 2B). The peak current amplitude remained little changed by deltamethrin, although the threshold for activation was shifted by ~−10 to −15 mV. Such a shift in activation is commonly found for mammalian Na^+ channels after insecticide treatment (e.g., Tatebayashi and Narahashi, 1994). A small fraction of peak Na^+ currents became noninactivating and maintained during the test pulse. Slow-decaying tail currents appeared after repolarization but were evident only at higher test pulses (arrows). The amplitude of this slow-decaying tail current was rather small compared with the peak current amplitude. The overall current kinetics of Nav1.4-I687M (Fig. 2C) remained comparable with those of the Nav1.4 wild-type. The activation was leftward shifted significantly from those of the Nav1.4 wild-type (by −17.1 mV in $V_{0.5}$; Table 1, $p < 0.05$) but the steady-state inactivation parameter was little changed (by −0.7 mV in $h_{0.5}$). As expected, the effects of 10 μM deltamethrin in Nav1.4-I687M mutant channels were greater than those found in wild-type (Fig. 2D). The relative maintained current in Nav1.4-I687M mutant was about 2- to 3-fold larger than that in wild-type. For comparison, we also replaced the methionine residue with threonine as in *para superkdr* mutants. The overall current kinetics of Nav1.4-I687T mutant channels were also comparable with those of wild-type channels (Fig. 2E). The activation and the inactivation parameters were listed in Table 1 along with those of wild-type and Nav1.4-I687M channels. However, unlike Nav1.4-I687M, mutant Nav1.4-I687T channels became rather resistant to deltamethrin at 10 μM (Fig. 2F). Thus, a point mutation from isoleucine to methionine, but not to threonine, at position I687 renders the Nav1.4 channels more sensitive than the wild-type channels to deltamethrin.

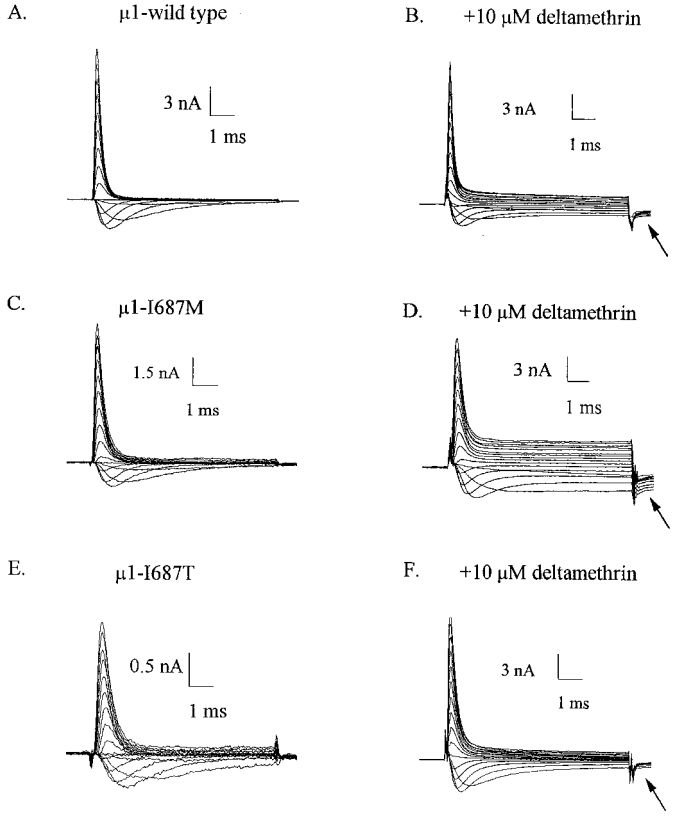

Fig. 2. Activation of Nav1.4 wild-type and mutant channels with and without deltamethrin. Cells were first dialyzed with internal solution for ~20 to 30 min. Superimposed Na^+ current families elicited by 8-ms test pulses ranging from −70 to +80 mV were shown in A, C, and E, without deltamethrin. Pulses were delivered every 10 s in 10-mV increments from a holding potential of −140 mV. The traces in B, D, and F were collected in the presence of 10 μM deltamethrin. The P/−4 method after the pulse was not used to collect these data, as the tail current appeared during this time. Maximal leak currents were generally minimal (<0.3 nA). The arrows on the traces indicate the drug-induced slow tail current. Membrane conductance (g_m) was calculated from the equation $g_m = I_{Na} / (E_m - E_{Na})$, where I_{Na} is the peak current elicited by the test pulse, E_m is the amplitude of the test pulse, and E_{Na} is the estimated reversal potential. Data were normalized with respect to the current evoked by the test pulse of +40 mV and fitted to a Boltzmann equation: $1 / [1 + \exp((V_{0.5} - V / k_a)])$. The average midpoint voltage ($V_{0.5}$) and slope factor (k_a) for mutant and wild-type channels are listed in Table 1.

The modifications of Nav1.4-I687M Na^+ currents by 10 μM deltamethrin were drastically enhanced by repetitive pulses. Figure 3A shows the comparison of superimposed current traces of Nav1.4 wild-type, Nav1.4-I687M, and Nav1.4-I687T mutant channels after repetitive pulses. Pulses applied at 2 Hz did not significantly enhance modifications of wild-type and Nav1.4-I687T mutant channels (Fig. 3A, left and right), whereas an identical pulse protocol greatly altered the current kinetics of Nav1.4-I687M (middle). First, the noninactivating current increases with each additional pulse until it reaches a steady-state level at 20 to 30 pulses. Second, tail currents appeared after repolarization and their amplitude greatly increased with each additional pulse until reaching a maximal steady-state level around 20 to 30 pulses. Stimulation with 100 brief conditioning pulses at a higher frequency induced tail currents in I687M mutant channels that decayed slowly and took more than 30 s to complete (Fig. 3B; center). The time constant for the decay of Nav1.4-I687M tail current was ~10 s, 30-fold slower than that of the wild-type (~0.3 s; Fig. 3B; left). The tail current for Nav1.4-I687T under the

same pulse protocol was small, and its time constant was fast (~0.07 s; Fig. 3B, right). The time constant values of ~0.3 s and ~0.07 s for the tail current decay in Nav1.4 wild-type and Nav1.4-I687T mutant channels, respectively, readily explain the lack of additional modifications by deltamethrin during repetitive pulses at 2 Hz (Fig. 3A, right and left). Such a rapid decay in tail currents prevents cumulative effects by repetitive pulses at 2 Hz (i.e., 0.5 s per pulse).

Batrachotoxin Modifies the I687M Na^+ Mutant Channel and Enhances Binding of Deltamethrin. BTX modified wild-type and Nav1.4-I687M mutant channels in a similar manner. Repetitive pulses of +50 mV for 21 ms facilitated the binding of BTX and consequently elicited noninactivating maintained currents during depolarization (Fig. 4A and B). Application of 1000 pulses sufficed to modify a significant fraction of the Na^+ current (≥80%) that becomes noninactivating during depolarization. A small reduction in the peak current occurred during repetitive pulses, probably because of the cumulative effect of the Na^+ channel slow inactivation. Unlike deltamethrin, BTX did not induce slow-decaying tail currents upon repolarization to −140 mV in either wild-type or Nav1.4-I687M mutant channels; only the fast-decaying tail currents (Fig. 4, dotted arrows) were present, which corresponded to the rapid closing of open BTX-modified channels. Thus, point mutation at Nav1.4-I687M did not affect BTX binding.

To test whether deltamethrin remains effective in binding with BTX-modified Nav1.4-I687M Na^+ channels, we first included 5 μM BTX in the pipette solution and applied ~600 repetitive pulses to facilitate BTX binding. Because bound BTX did not dissociate from its receptor site under our experimental conditions, we subsequently applied 10 μM deltamethrin externally after BTX modifications became evident. Figure 5A shows that deltamethrin remained active in BTX-modified Nav1.4-I687M channels and elicited tail currents that clearly were larger in amplitude than those from wild-type. The control current (trace 1) was taken first, followed by traces 2 and 3 upon treatment of 10 μM deltamethrin for 5 and 6 min, respectively. Notice that the tail current decayed slowly and a portion of it remained even

TABLE 1

Parameters for activation and steady-state inactivation of Nav1.4 wild-type and mutant Na^+ channels

The values for the voltage dependence of activation $V_{0.5}$ and k_a (mean ± S.E. of the fit) were obtained as described in the legend to Fig. 2. For steady-state inactivation, standard h_∞ curves were constructed (Nau et al., 1999). Pulses were administered at 10-s intervals. The midpoint voltage for steady-state inactivation ($h_{0.5}$) and the slope factor (k_h) values are presented as mean ± S.E.M.

		Channel Types				
		Nav 1.4-wt	I687M	I687T	I687M/N784K	I687M/F1278I
Activation	$V_{0.5}$ (mV)	−32.1 ± 0.8	−49.2 ± 1.0*	−41.6 ± 1.7*	−54.2 ± 1.7*	−40.2 ± 1.5*
	k_a (mV)	11.5 ± 0.7	9.6 ± 0.9	10.5 ± 1.6	10.8 ± 1.6	8.9 ± 1.4
		(n = 5)	(n = 5)	(n = 6)	(n = 5)	(n = 6)
Steady-State Inactivation	$h_{0.5}$ (mV)	−88.5 ± 2.4	−89.2 ± 2.1	−82.1 ± 2.1	−90.8 ± 1.8	−85.1 ± 4.6
	k_h (mV)	6.5 ± 0.3	7.1 ± 0.2	6.9 ± 0.5	5.6 ± 0.1*	6.4 ± 0.3
		(n = 5)	(n = 5)	(n = 6)	(n = 5)	(n = 4)

* $P < 0.05$.

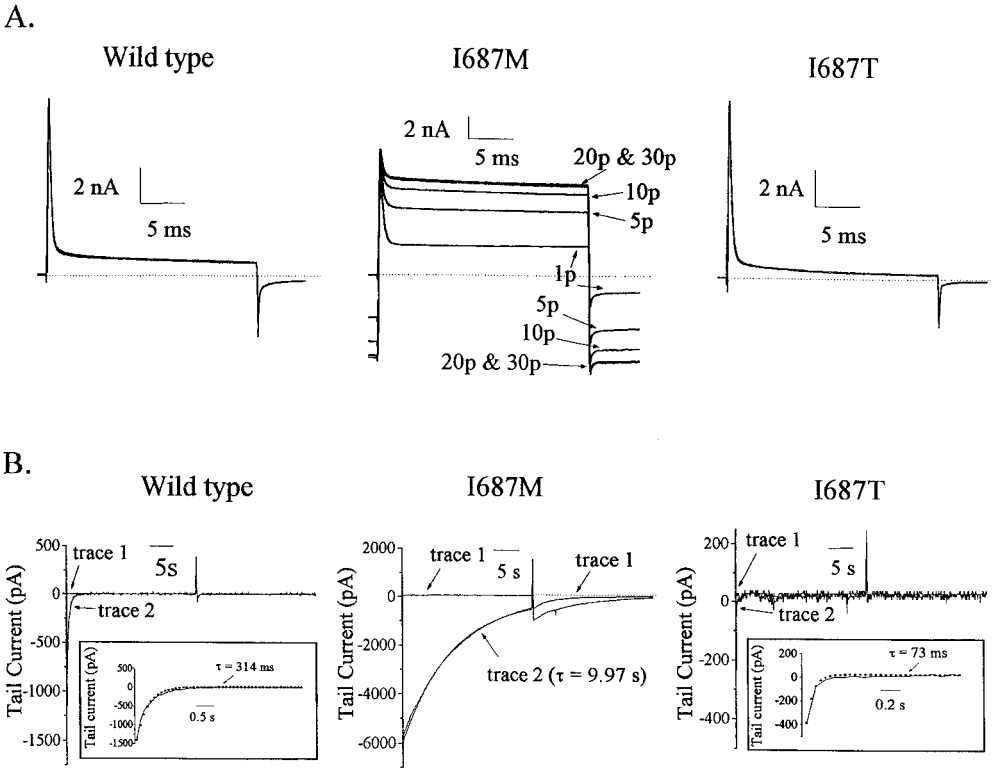

Fig. 3. Modification of Nav1.4 wild-type and mutant channels by 10 μM deltamethrin with repetitive pulses. A, superimposed traces of Na^+ currents in the presence of 10 μM deltamethrin after repetitive pulses. Cells were held at −140 mV and subjected to 30 depolarizations to +30 mV for 24 ms at 2 Hz. Notice that deltamethrin elicited a use-dependent effect in the I687M mutant. The numbers correspond to the number of pulses applied. B, Nav1.4 wild-type and mutant tail currents induced by 10 μM deltamethrin with (trace 2) and without (trace 1) a rapid train of 100 pulses (+30 mV for 3 ms at 10 Hz). The cells were then held at −140 mV and the tail currents recorded for 25 s, followed by a 100-ms test pulse to +30 mV. Repetitive depolarizations produced an augmented tail current to various extents in all channels (trace 2 versus trace 1). Note that the tail current of the I687M (τ = 9.2 ± 0.84 s, n = 6) mutant decays slowly relative to the Nav1.4 wild-type (τ = 304 ± 16 ms, n = 5) and I687T (τ = 70 ± 5 ms, n = 5) mutant channels. An inset for trace 2 with a faster time frame is provided when appropriate.

before the pulse of trace 3. Little or no increase in slow-tail current amplitude was found thereafter. Evidently, the wash-in kinetics of deltamethrin was much faster than that of wild-type and Nav1.4-I687M mutant channels without BTX (<10 min versus >30 min). Again, repetitive pulses (+50 mV for 5 ms at 20 Hz) enhanced both the maintained current amplitude during the pulse and the tail current amplitude after repolarization (Fig. 5B). The time course of the decay of the slow tail current component was measured under a slower time frame with a time constant of 28.7 s (Fig. 5C). These results together suggested that BTX enhanced the binding of deltamethrin by slowing its dissociation rate and that the BTX and the deltamethrin receptors were distinct and probably separated in situ at two different binding sites. The enhancement of deltamethrin binding by BTX was therefore due to an "allosteric" mechanism. Deltamethrin might also enhance the binding of BTX reciprocally because the maintained current amplitude was increased. It is noteworthy that the maintained current came from the BTX-modified channels, the deltamethrin-modified channels, and the channels modified by both ligands. In contrast, the slowly decay-

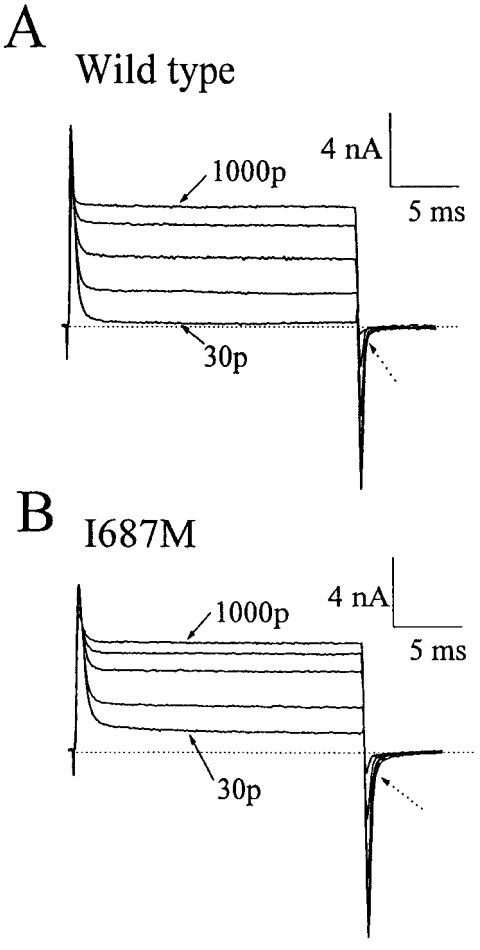

Fig. 4. BTX-sensitive phenotype in Nav1.4-I687M mutant channels. Superimposed current traces were recorded from wild-type (A) and I687M (B) mutant channels during repetitive pulses at +50 mV for 21 ms at 2 Hz. Cells were held at −140 mV and dialyzed for 15 min before repetitive pulses. BTX modifies both channel types effectively (n = 5). Dotted arrows indicate the fast decaying tail current, while the solid arrows show maintained currents during the repetitive pulse of 30, 100, 300, 600, and 1000; traces 30p and 1000p are labeled. The straight dotted line indicates the current baseline.

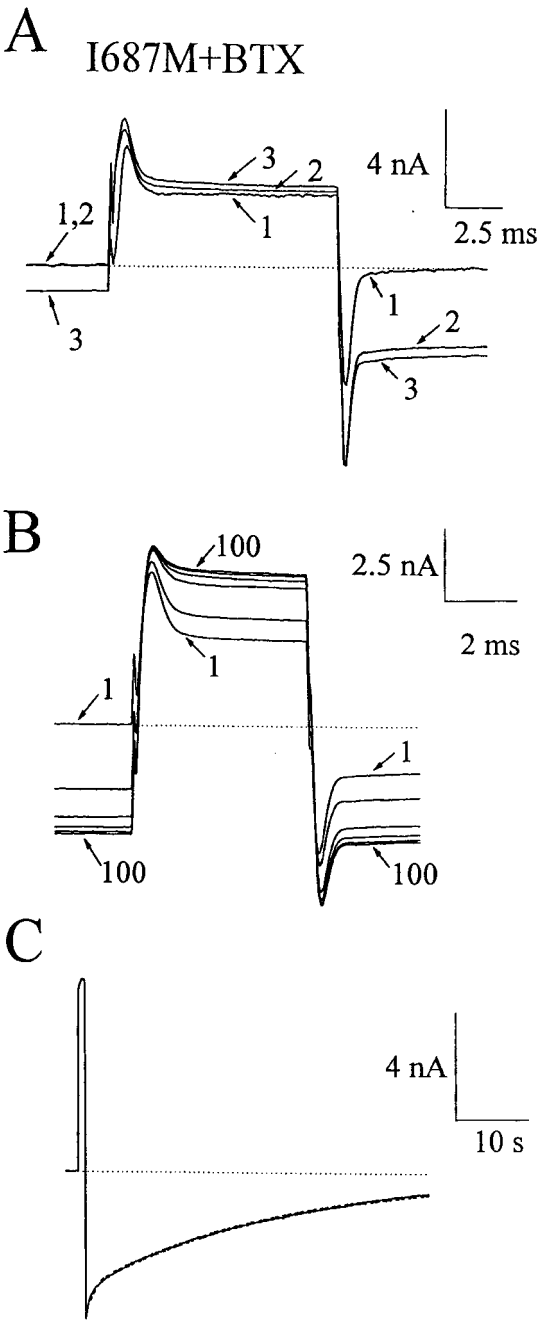

Fig. 5. Deltamethrin binding in BTX-modified Nav1.4-I687M mutant channels. A, superimposed current traces in Nav1.4-I687M mutant channels already modified by BTX were recorded before (trace 1), 5 min after (trace 2), and 6 min after (trace 3) 10 μM deltamethrin superfusion. Trace 1 was taken after 600 repetitive pulses (as described in the legend to Fig. 4) that were applied to facilitate BTX binding. BTX at 5 μM was included in the pipette solution. Notice that the tail current appeared readily 5 min after the application of deltamethrin. This tail current decayed very slowly at −140 mV and the residual tail current remained even 1 min after repolarization (trace 3, front). The straight dotted line indicates the current baseline. B, repetitive pulses of +50 mV for 5-ms at 20 Hz further enhanced deltamethrin binding; both the maintained current and slow tail current amplitudes were significantly increased. Currents from pulse numbers 1, 5, 30, 50, 75, and 100 were superimposed for comparison. C, a prolonged depolarization for 1 s to +50 mV was applied to generate the tail current. The maintained Na^+ current during the pulse and the tail current upon repolarization to −140 mV were recorded at a slower time frame. The decay of the slow tail current was well fitted by a single exponential function (dotted fit).

ing tail current ($\tau = 26.5 \pm 2.3$ sec, $n = 5$) probably came from channels modified by both ligands exclusively, whereas the remaining decaying tail current could come from channels modified by deltamethrin alone.

Residue F1278 at D3-S6 Is Critical for Deltamethrin Action. An additional point mutation of Nav1.4-I687M at the segment D3-S6, Nav1.4-F1278I, drastically hampered the effects of deltamethrin on Na^+ current kinetics. Figure 6A (left) shows the family of superimposed Na^+ current traces from Nav1.4-I687M/F1278I mutant at various voltages before and after 10 μM deltamethrin (left versus right). The activation and inactivation parameters were measured and are listed in Table 1 for comparison with wild-type and with other mutants. Unlike Nav1.4-I687M channels, the phenotype of Nav1.4-I687M/F1278I channels after deltamethrin treatment became comparable with that of Nav1.4-I687T (Fig. 6A; right). Repetitive pulses using the same pulse protocol described in Fig. 3 did not enhance modifications of current kinetics of this mutant by 10 μM deltamethrin (Fig. 6C). There were no visible slow-decaying tail currents even after 100 brief conditioning pulses under a higher frequency (Fig. 6D). The fast- decaying tail had an average time constant of 0.06 s, which is not statistically different from ~0.07 s for Nav1.4-I687T ($P = 0.65$). Quantitative analyses of maintained currents before and after repetitive pulses at 2 Hz are included in Fig. 7. Clearly, Nav1.4-I687M/F1278I channels showed a rather resistant phenotype to deltamethrin as compared with Nav1.4-I687M channels, demonstrating that the residue at F1278 was critical for pyrethroid action.

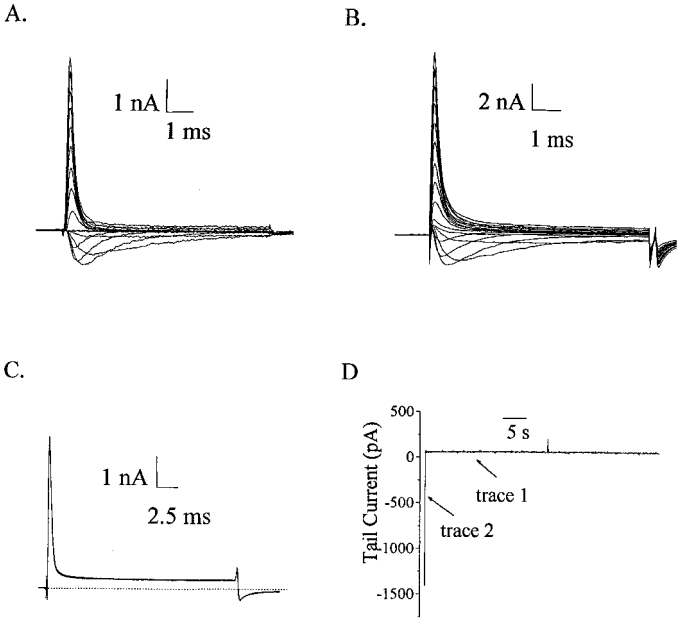

Fig. 6. Deltamethrin-resistant phenotype in Nav1.4-I687M/F1278I mutant channels. Superimposed Na^+ current families were measured as described in Fig. 2 in the absence (A) and in the presence (B) of 10 μM deltamethrin. C, superimposed traces of Na^+ currents in the presence of 10 μM deltamethrin after repetitive depolarizing pulses as described in Fig. 3A. Cells were maintained at a holding potential of −140 mV and were subjected to 30 pulses to +30 mV for 24 ms at 2Hz. Notice that deltamethrin elicits no use-dependent effect in I687M/F1278I mutant channels. D, tail currents of the I687M/F1278I mutant induced by 10 μM deltamethrin with (trace 2) and without (trace 1) a conditioning train of 100 brief depolarizing pulses at ~10 Hz as described in Fig. 3B. No slow tail currents were present.

F1278 at D3-S6 Is Not Critical for Batrachotoxin Action. To test whether BTX action is affected by the point mutation at F1278 position, we included 5 μM BTX in the pipette solution and applied repetitive pulses as described in Fig. 4 to facilitate BTX binding in Nav1.4-I687M/F1278I mutant channels. Figure 8A shows that BTX readily modifies the Nav1.4-I687M/F1278I mutant channels. Application of 1000 pulses converted a large fraction of Na^+ current into a noninactivating component during depolarization. Tail cur-

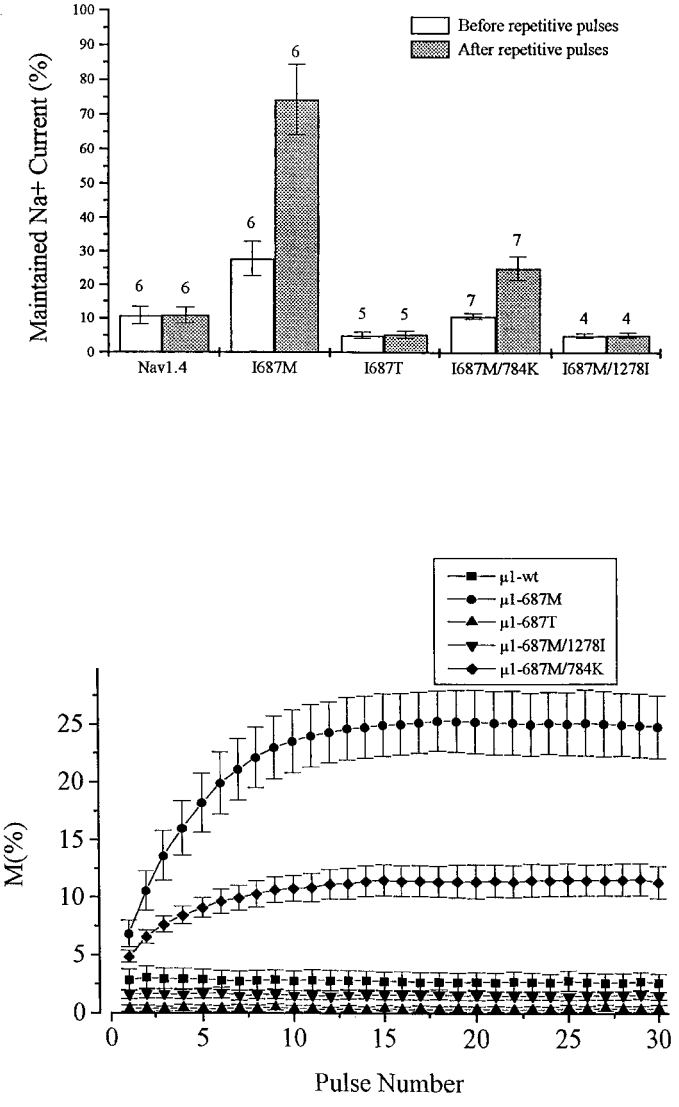

Fig. 7. Quantitative analyses of Nav1.4-wild-type and mutant channels modified by 10 μM deltamethrin. A, in the presence of 10 μM deltamethrin, the maintained currents were measured near the end of the depolarization, both before and after repetitive pulsing as described in Fig. 3A. These values were then normalized with respect to the peak current of the same trace and plotted against the mutant type. The number of experiments for each channel type is shown above each bar graph. B, the percentage (M) of channels modified by 10 μM deltamethrin was plotted against the number of depolarizing pulses. Cells were subjected to repetitive pulses as described in Fig. 3A. The percentage of modified channels (M) was calculated from the equation $M = [\{I_{tail} / (E_{tail} - E_{Na})\}/\{I_{Na} / (E_m - E_{Na})\}] \times 100$, where I_{tail} is the tail current amplitude, E_{tail} is the voltage potential at which the tail current was recorded (−140 mv), E_{Na} is the estimated reversal potential of the Na^+ current, and I_{Na} is the amplitude of the peak current elicited by the test pulse. Five, six, five, four, and seven experiments were performed for Nav1.4 wild-type, I687M, I697T, I687M/784K, and I697M/1278I, respectively.

rents in the Nav1.4-I687M/F1278I mutant decayed rapidly (dotted arrow), as in the wild-type channels. Therefore, the BTX action in Nav1.4-I687M/F1278I mutant channels remained little affected. It is interesting that the binding of BTX did not reverse the mutant channel from its deltamethrin-resistant phenotype. Figure 8B shows that little or no slow tail current in the BTX-modified Na^+ channels appears after 10 μM external deltamethrin application even after continuous drug perfusion of the cell for 30 to 45 min (dotted arrow). Further repetitive pulses also failed to elicit any slow tail currents upon repolarization (Fig. 8C). These phenotypes were repeated in four separate experiments and contrasted sharply with the phenotype found in Nav1.4-I687M (described in Fig. 5), further confirming that the BTX receptor and the deltamethrin receptor were distinct and that BTX could not rescue the F1278I mutational defect in deltamethrin binding.

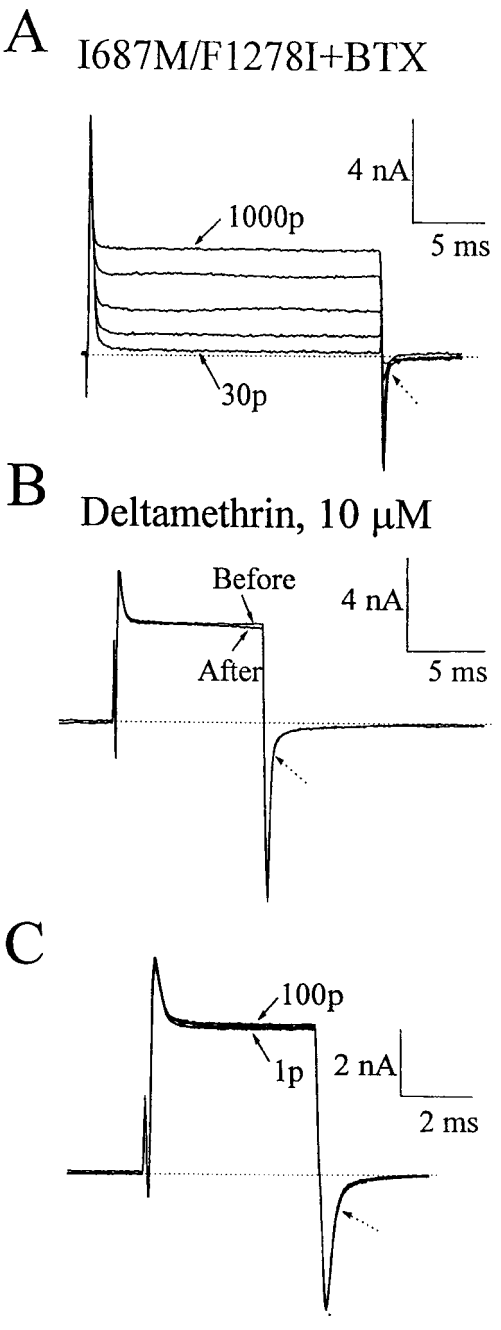

Fig. 8. BTX-sensitive phenotype in Nav1.4-I687M/F1278I mutant channels. A, superimposed Na^+ currents in Nav1.4-I687M/F1278I mutant channels were recorded during repetitive pulses of +50 mV for 21 ms at 2 Hz as described in the legend to Fig. 4. Nav1.4-I687M/F1278I mutant channels remained sensitive to BTX at 5 μM; maintained currents were evident and became progressively larger during repetitive pulses. Currents from pulse number 30, 100, 300, 600, and 1000 were shown. B, superimposed current traces in BTX-modified Nav1.4-I687M/F1278I mutant channels before and after application of 10 μM deltamethrin for 30 min show that the insecticide failed to elicit any slow tail current (dotted arrow). The pulse protocol was the same as described in Fig. 5A. C, after 30-min superfusion of 10 μM deltamethrin, repetitive pulses of +50 mV for 5 ms at 20 Hz were subsequently applied in BTX-modified Nav1.4-I687M/F1278I mutant channels as described in Fig. 5B. Again, no slow tail current was evident under these conditions.

N784K at D2-S6 Modulates Deltamethrin Action. We attempted to study the known *kdr* mutation at the D2-S6 homologous site, L785F, in Nav1.4-I687M channels. Unfortunately, we repeatedly failed to detect sufficient currents in HEK293t cells transfected with the Nav1.4-I687M/L785F mutant or with the Nav1.4-I687M/L785K mutant. An adjacent site, N784, was reported to be critical for BTX action; lysine substitution of N784 rendered the mutant channel completely resistant to 5 μM BTX (Wang et al., 2001). We found that the Nav1.4-I687M/N784K mutant expressed sufficient Na^+ currents for insecticide studies (Fig. 9A). This mutant channel was also completely resistant to 5 μM BTX; repetitive pulses of 1000 at 2 Hz failed to modify the current kinetics. The activation and inactivation parameters were measured and are listed in Table 1. Figure 9B shows that the Nav1.4-I687M/L784K channels are nevertheless modified by 10 μM deltamethrin. Repetitive pulses further enhanced the modification significantly (Fig. 9C). Quantitative analyses of maintained currents before and after repetitive pulses showed that sensitivity of this mutant to deltamethrin fell

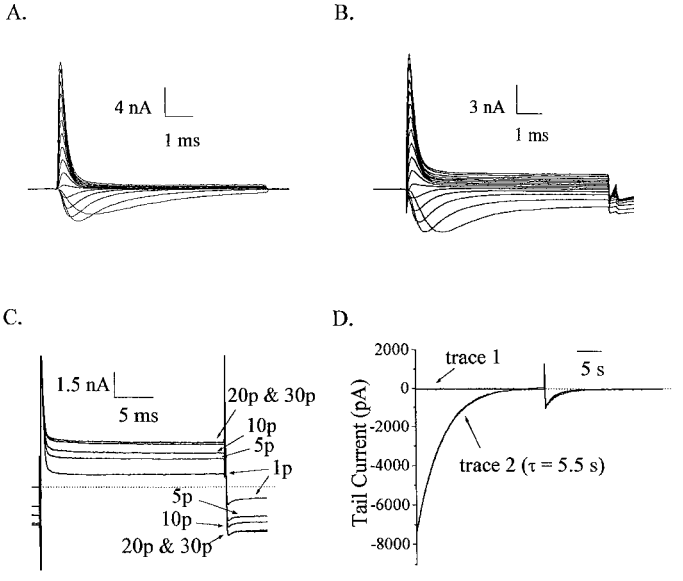

Fig. 9. Partial deltamethrin-resistant phenotype in I697M/N784K mutant channels. Superimposed Na^+ current families of I687M/N784K mutant channels in the absence (A) and presence (B) of 10 μM deltamethrin were recorded as described in Fig. 2. C, superimposed traces of Na^+ currents in the presence of 10 μM deltamethrin were recorded during 30 repetitive depolarizations to +30 mV for 24 ms at 2Hz as described in Fig. 3A. Cells were held at −140 mV. The numbers labeled correspond to the number of pulses applied. D, I687M/784K mutant tail currents induced by 10 μM deltamethrin with (trace 2) and without (trace 1) a conditioning train of brief pulses (+30 mV for 3 ms) at ~10Hz as described in Fig. 3B.

between those of the μ1-I687M mutant and the Nav1.4-I687M/F1278I mutant (Fig. 7). In addition, the tail current of the Nav1.4-I687M/F1278I mutant induced by repetitive pulses appeared to decay faster than that of the Nav1.4-I687M mutant (Fig. 9D; τ = 5.5 s versus 10.0 s). This phenotype remained the same with or without 5 μM BTX in the pipette solution. These results together demonstrated that residue N784K modulated the binding of deltamethrin but did not eliminate it, consistent with the notion that N784 was adjacent to but not necessarily a part of the deltamethrin binding site.

Discussion

This report describes three principal findings. First, an I687M background mutation of rat skeletal muscle Nav1.4 Na^+ channels increases their deltamethrin sensitivity in HEK293t cells, whereas the I687T mutation has the opposite effect. Second, an additional F1278I mutation at segment D3-S6 renders Nav1.4-I687M/F1278I channels resistant to deltamethrin. Third, a lysine substitution of residue N784 at segment D2-S6 significantly reduces the deltamethrin effects on Nav1.4-I687M/N784K channels. Implications of these results are discussed below.

Are Nav1.4 Channels Expressed in HEK293t Cells Applicable for Insecticide Studies? Deltamethrin appears as a weak gating modifier of the Nav1.4 channel in HEK293t cells; even at 10 μM, its effects on the Nav1.4 wild-type channels are unremarkable (Fig. 2). The maintained current during depolarization is ~10% of its peak current amplitude; this level of modification is comparable with rat brain channels expressed in *Xenopus laevis* oocytes (Vais et al., 2000a). The induced tail current after repolarization to the holding potential is also small in amplitude and corresponds to ~3% of the total channels. In addition, the time to reach the steady-state modification requires more than 30 to 40 min of continuous drug perfusion. The low solubility of deltamethrin and its long wash-in time make the dose-response study impractical in Nav1.4 channels. Repetitive pulses at 2 Hz to improve deltamethrin binding with the open Na^+ channel are also fruitless.

However, a background mutation, Nav1.4-I687M, greatly improved the level of gating modification by deltamethrin. Such a strategy was used previously by Vais et al. (2000a) for the Nav1.2 channel expressed in oocytes. With this mutation, the maintained current corresponds to ~28% of the peak amplitude, and the induced tail current corresponds to ~7% of Nav1.4-I687M channels modified by deltamethrin. Repetitive pulses increase the maintained current to ~75% and the tail current to ~25% of total channels modified. The discrepancy between the amount of deltamethrin-modified Nav1.4-I687M channels in maintained and in tail currents is disconcerting but can be explained. Vais et al. (2000b) found that the tail current was rectified when the voltage was more negative than −80 mV, probably because of the blockade of tail current by external calcium ions. At −140 mV holding potential, deltamethrin-induced tail currents would be greatly rectified in our assay and underestimated. Nonetheless, the end result indicates that I687M mutation causes an ~8-fold increase in the gating modification of the Nav1.4 channels by deltamethrin. With this level of modification, Nav1.4-I687M channels became useful for insecticide studies in HEK293t cells, including the mapping of the deltamethrin receptor. In *Xenopus laevis* oocytes, homologous substitution of the rat Nav1.2-I874 M channel caused a 80% gating modification by 1 μM deltamethrin (5 ms pulses at ~60 Hz; Vais et al., 2000a). Beside experimental protocols, this quantitative difference could be caused by distinct Na^+ channel isoforms and/or different expression systems.

Does the D3-S6 Segment Form a Part of the Insecticide Receptor? The double mutations of Nav1.4-I687M/F1278I reversed the Nav1.4-I687M channel from a deltamethrin-sensitive to a deltamethrin-resistant phenotype. Quantitative analyses of maintained and tail currents reveal that Nav1.4-I687M/F1278I mutant is less sensitive to deltamethrin than the Nav1.4 wild-type and is as resistant as Nav1.4-I687T, a *superkdr* mutation. The fact that the Nav1.4-I687M/F1278I mutant confers the deltamethrin-resistant phenotype directly supports the genetic analysis of tick insecticide-resistant Na^+ channel by He et al. (1999). We noticed that point mutations often change the channel gating parameters in varying degrees (Table 1). Whether such gating changes also contribute to insecticide resistance in vivo is unclear. Final confirmation of this insecticide-resistant phenotype in tick Na^+ channels is needed.

Although residue Nav1.4-F1278 is critical for insecticide action, this result may be interpreted in two different ways. First, residue F1278 may indirectly affect the insecticide binding in the Nav1.4 channel. Second, residue F1278 may form a part of the insecticide receptor. Residue F1278 is at position 15 within D3-S6, and residue L785, a *kdr* allele, is at position 14 within D2-S6 (Fig. 1). If L785 forms a part of the insecticide receptor (Vais et al., 2000b), it is probable that residue F1278 aligns closely with residue L785 (Lipkind and Fozzard, 2000). Such close alignment may allow deltamethrin to interact directly with both residues. In fact, this in situ space between D2-S6 and D3-S6 may not be optimal for the insecticide binding. Repetitive pulses may widen or reorient this in situ space during gating transitions and increase the insecticide binding with the open form of the channel. The suggestion of the existence of a domain-interface receptor for insecticides that includes segments of D2-S6 and D3-S6 is appealing. Specifically, it provides the structural basis for deltamethrin action under Hille's modulated receptor hypothesis (Hille, 1992). A domain-interface receptor situated along the "moving" S6 segments (Yellen, 1998; Perozo et al., 1999) may explain the complicated consequences of deltamethrin poisoning. For example, the reason for the appearance of maintained current and induced tail current could be the stabilization of multiple S6 segments in their open configuration by deltamethrin binding.

Is the Insecticide Receptor Separated from the BTX Receptor at D3-S6? Residues at D3-S6 probably form a part of receptor for BTX (Wang et al., 2000). The BTX receptor seems to include two residues at position S1276 and L1280. The α-helical S6 model indicates that these residues face the opposite side of residue F1278 (i.e., ~100° per residue or 3.6 residues per α-helical turn; Fig. 1C). Not surprisingly, therefore, deltamethrin interacts with BTX-modified Nav1.4-I687M channels and its binding seems to be enhanced by BTX. This enhancement is reflected in the slower tail current decay and in the faster wash-in time (30–40 min versus <10 min). This result demonstrates that BTX enhances the insecticide binding. The reverse was also reported (Lombet et al.,

1988; Trainer et al., 1993). In addition, BTX binds readily with the Nav1.4-I687M/F1278I channel but fails to rescue its deltamethrin-resistant phenotype. Thus, distinct residues in D3-S6 may form a part of receptors for BTX and for deltamethrin and these two receptors are situated at the opposite face of the D3-S6 α-helical structure (Fig. 1C).

Is the Insecticide Receptor at D2-S6 Segment Adjacent to the BTX Receptor? The *kdr* allele, residue Nav1.4-L785 within D2-S6, is located next to N784, which was identified as a part of the putative BTX receptor (Wang et al., 2001). If BTX and insecticide receptors are located closely enough within D2-S6, could a mutation at N784 affect the deltamethrin binding? We found that Nav1.4-I687M/N784K displays a partially resistant phenotype (Fig. 7). This result supports that the insecticide receptor at D2-S6 is adjacent to the BTX receptor. Unfortunately, we failed to express mutant Nav1.4-I687M/L785F or Nav1.4-I687M/L785K and therefore cannot determine their BTX and deltamethrin phenotypes. Our previous report, however, demonstrated that the L785K mutant remained sensitive to 5 μM BTX (Wang et al., 2001), suggesting that the *kdr* allele is not a part of the BTX receptor. For comparisons, the time constant of the deltamethrin-induced tail current decay follows this order (mean ± S.E.M., n = 4–6): Nav1.4-I687M (9.2 ± 0.8 s) > Nav1.4-I687M/N784K (4.7 ± 0.6 s) > Nav1.4 (0.30 ± 0.02 s) > Nav1.4-I687T (0.07 ± 0.01 s) ≈ Nav1.4-I687M/F1278I (0.06 ± 0.02 s). In addition, BTX slows the time constant of Nav1.4-I687M from 9.2 to 28.7 s. These values probably reflect the dissociation rate of deltamethrin from its receptor at the holding potential and may represent the best indicator for their relative potency toward Nav1.4 mutant channels.

Finally, two recent reports suggest that residue I/v433 may form part of an insecticide receptor within D1-S6 (Fig. 1B; Zhao et al., 2000; Lee and Soderlund, 2001). This position has been proposed as part of the BTX receptor. However, the effect of *kdr* allele on insecticide action is more profound than that of the *para*-V421 M (Nav1.4-I433, Zhao et al., 2000). This phenotype, therefore, is similar to that found in Nav1.4-I687M/N784K. Consequently, it remains unclear whether this position is contiguous or is a part of the insecticide receptor.

In summary, we hypothesize that the residue at the Nav1.4-F1278 position forms a part of the insecticide receptor, which is located at the opposite surface of the α-helical D3-S6 structure away from the putative BTX receptor. Substitution of F to I could disrupt its binding with deltamethrin directly. However, an indirect mutational effect could also account for these results. In addition, as a part of the putative BTX receptor, residue N784K at the D2-S6 segment modulates the deltamethrin binding, probably because this residue is adjacent to position L785 (a *kdr* allele), which may form a part of the "interdomain" insecticide receptor along with residue F1271 at D3-S6. It is noteworthy that a separate insecticide receptor within a different S6 segment is equally possible. This would agree with the finding that *superkdr* mutations reduce the number of deltamethrin binding sites per channel from two to one (Vais et al., 2000b). In any event, the similar pharmacological profiles for insecticides and BTX as Na^+ channel activators are probably derived from their linkage with respect to S6 movements during gating, as proposed previously for BTX action (Wang et al., 2000; 2001).

References

Bloomquist JR and Miller TA (1986) Sodium channel neurotoxins as probes of the knockdown resistance mechanism. *Neurotoxicology* **7:**217–223.

Cannon SC and Strittmatter SM (1993) Functional expression of sodium channel mutations identified in families with periodic paralysis. *Neuron* **10:**317–326.

Catterall WA (2000) From ionic currents to molecular mechanisms: the structure and function of voltage-gated sodium channels. *Neuron* **26:**13–25.

Cota G and Armstrong CM (1989) Sodium channel gating in clonal pituitary cells: the inactivation step is not voltage dependent. *J Gen Physiol* **94:**213–232.

Doyle DA, Cabral JM, Pfuetzner RA, Kuo A, Gulbis J, Cohen S, Chait BT and MacKinnon R (1998) The structure of the potassium channel: molecular basis of potassium conduction and selectivity. *Science (Wash DC)* **280:**69–77.

Hamill OP, Marty E, Neher ME, Sakmann B and Sigworth FJ (1981) Improved patch-clamp techniques for high-resolution current recording from cells and cell-free membrane patches. *Pfluegers Arch* **391:**85–100.

He H, Chen AC, Davey RB, Ivie GW and George JE (1999) Identification of a point mutation in the para-type sodium channel gene from a pyrethroid-resistant cattle tick. *Biochem Biophys Res Commun* **261:**558–561.

Hille B (1992) Modifiers of gating, in *Ionic Channels of Excitable Membranes*, pp. 445–471, Sinauer Associates Inc., Sunderland, Massachusetts.

Lee SH and Soderlund DM (2001) The V410M mutation associated with pyrethroid resistance in *Heliothis virescens* reduces the pyrethroid sensitivity of house fly sodium channels expressed in *Xenopus* oocytes. *Insect Biochem Mol Biol* **31:**19–29.

Linford NJ, Cantrell AR, Qu Y, Scheuer T and Catterall WA (1998) Interaction of batrachotoxin with the local anesthetic receptor site in transmembrane segment IVS6 of the voltage-gated sodium channel. *Proc Natl Acad Sci USA* **95:**13947–13952.

Lipkind GM and Fozzard HA (2000) KcsA crystal structure as framework for a molecular model of the Na^+ channel pore. *Biochemistry* **39:**8161–8170.

Lombet A, Mourre C and Lazdunski M (1988) Interaction of insecticides of the pyrethroid family with specific binding sites on the voltage-dependent sodium channel from mammalian brain. *Brain Res* **459:**44–53.

Miyazaki M, Ohyama K, Dunlap DY and Matsuo H (1996) Cloning and sequencing of the *para* -type sodium channel gene from susceptible and *kdr* -resistant German cockroaches (*Blattella germanica*) and housefly (*Musca domestica*). *Mol Gen Genet* **252:**61–68.

Narahashi T (1992) Nerve membrane Na^+ channels as targets of insecticides. *Trends Pharmacol Sci* **13:**236–241.

Nau C, Wang S-Y, Strichartz GR and Wang GK (1999) Point mutations at N434 in D1–S6 of μ1 Na^+ channels modulate potency and stereoselectivity of local anesthetic enantiomers. *Mol Pharmacol* **56:**404–413.

Pauron D, Barhanin J, Amichot M, Pralavorio M, Berge JB and Lazdunski M (1989) Pyrethroid receptor in the insect Na^+ channel: alternation of its properties in pyrethroid resistant flies. *Biochemistry* **28:**1673–1677.

Perozo E, Cortes DM and Cuello LG (1999) Structural rearrangements underlying K^+-channel activation gating. *Science (Wash DC)* **285:**73–78.

Tatebayashi H and Narahashi T (1994) Differential mechanism of action of the pyrethroid tetramethrin on tetrodotoxin-sensitive and tetrodotoxin-resistant sodium channels. *J Pharmacol Exp Ther* **270:**595–603.

Trainer VL, Moreau E, Guedin D, Baden DG and Catterall WA (1993) Neurotoxin binding and allosteric modulation at receptor sites 2 and 5 on purified and reconstituted rat brain sodium channels. *J Biol Chem* **268:**17114–17119.

Vais H, Atkinson S, Eldursi N, Devonshire AL, Williamson MS and Usherwood PN (2000a) A single amino acid change makes a rat neuronal sodium channel highly sensitive to pyrethroid insecticides. *FEBS Lett* **470:**135–138.

Vais H, Williamson MS, Goodson SJ, Devonshire AL, Warmke JW, Usherwood PN and Cohen CJ (2000b) Activation of *Drosophila* sodium channels promotes modification by deltamethrin. Reductions in affinity caused by knock-down resistance mutations. *J Gen Physiol* **115:**305–318.

Wang S-Y, Barile M and Wang GK (2001) Disparate role of Na^+ channel D2–S6 residues in batrachotoxin and local anesthetic action. *Mol Pharmacol* **59:**1100–1107.

Wang S-Y, Nau C and Wang GK (2000) Residues in Na^+ channel D3–S6 segment modulate batrachotoxin as well as local anesthetic binding affinities. *Biophys J* **79:**1379–1387.

Wang S-Y and Wang GK (1998) Point mutations in segment I-S6 render voltage-gated Na^+ channels resistant to batrachotoxin. *Proc Natl Acad Sci USA* **95:**2653–2658.

Warmke JW, Reenan RA, Wang P, Qian S, Arena JP, Wang J, Wunderler D, Liu K, Kaczorowski GJ, Van der Ploeg L, Ganetzky B and Cohen CJ (1997) Functional expression of *Drosophila para* sodium channels: modulation by the membrane protein TipE and toxin pharmacology. *J Gen Physiol* **110:**119–133.

Williamson MS, Marinez-Torres D, Hick CA and Devonshire AL (1996) Identification of mutations in the housefly para-type sodium channel gene associated with knockdown resistance (kdr) to pyrethroid insecticides. *Mol Gen Genet* **252:**51–60.

Yellen G (1998) The moving parts of voltage-gated ion channels. *Q Rev Biophys* **31:**239–295.

Zhao Y, Park Y and Adams ME (2000) Functional and evolutionary consequences of pyrethroid resistance mutations in S6 transmembrane segments of a voltage-gated sodium channel. *Biochem Biophys Res Commun* **278:**516–521.

Zlotkin E (1999) The insect voltage-gated sodium channel as target of insecticides. *Annu Rev Entomol* **44:**429–455.

Address correspondence to: Dr. Ging Kuo Wang, Department of Anesthesia, Harvard Medical School and Brigham & Women's Hospital, 75 Francis St., Boston, MA, 02115. E-mail: wang@zeus.bwh.harvard.edu